European Journal of Pharmaceutics and Biopharmaceutics 70 (2008) 590–596

Contents lists available at ScienceDirect

European Journal of Pharmaceutics and Biopharmaceutics

journal homepage: www.elsevier.com/locate/ejpb

Research paper

Microcrystalline cellulose, a useful alternative for sucrose as a matrix former during freeze-drying of drug nanosuspensions – A case study with itraconazole

Van Eerdenbrugh Bernard [a], Vercruysse Sofie [a], Martens Johan A [b], Vermant Jan [c], Froyen Ludo [d], Van Humbeeck Jan [d], Van den Mooter Guy [a,*], Augustijns Patrick [a]

[a] Laboratory for Pharmacotechnology and Biopharmacy, Leuven, Belgium
[b] Center for Surface Chemistry and Catalysis, Heverlee, Belgium
[c] Department of Chemical Engineering, Heverlee, Belgium
[d] Metallurgy and Materials Engineering Department, Heverlee, Belgium

ARTICLE INFO

Article history:
Received 19 February 2008
Accepted in revised form 10 June 2008
Available online 18 June 2008

Keywords:
Media milling
Nanosuspensions
Freeze-drying
Sucrose
Microcrystalline cellulose
Itraconazole

ABSTRACT

Itraconazole nanosuspensions, stabilized with 10% TPGS (relative to the weight of itraconazole), were transformed into nanoparticulate powders by freeze-drying. The crystalline itraconazole nanoparticles showed peak broadening in the X-ray powder diffraction spectra and a lower melting point as inferred from differential scanning calorimetry. As it was found that freeze-drying compromised dissolution behavior, sucrose was added as a matrix, former (50,100 and 200%, relative to the weight of itraconazole). Higher amounts of sucrose unexpectedly resulted in a decrease in the dissolution rate. After thorough evaluation of the powders, it was found that whereas higher sucrose content showed a cryoprotective effect, agglomeration during the final phase of the subsequent drying step tended to increase with higher amounts of sucrose. Therefore, microcrystalline cellulose (MCC) was evaluated as an alternative matrix former. The inclusion of MCC resulted in fast dissolution that increased with increasing amounts of MCC [for powders containing 50%,100% and 200% MCC, (relative to the weight of itraconazole), the times required for 63.2% release were 10.5 ± 0.7, 6.4 ± 1.2 and 3.1 ± 0.5 min, respectively]. The dissolution profiles showed an initial phase of burst dissolution, followed by a phase of slower release. As the fraction showing burst dissolution increased with higher MCC content, the system holds promise to maintain the dissolution enhancing properties of nanoparticles in the dry form.

1. Introduction

Given the increasing number of compounds emerging from discovery programs having poor solubility and/or dissolution rate [1], pharmaceutical scientists are constantly seeking new formulation approaches in order to obtain an adequate oral bioavailability. Currently, novel possibilities are offered by the rapidly emerging field of nanoscience. One of the nanoscience approaches that has rapidly gained a proven record within the pharmaceutical sciences is the formulation of drugs as drug nanocrystals, having a size below 1 μm [2]. Characteristic for the nanocrystals is the very high specific surface area which can be expected to have a positive effect on the dissolution rate.

Drug nanocrystals can be obtained either by particle-size reduction (top–down approach) or by building up particles from a solution (bottom–up approach) [3]. Currently the former one is the standard technique, as witnessed by the fact that all of the five currently marketed products are based on this approach [4]. Within the group of the top–down techniques, media milling is the most popular technology and 4 of the 5 currently marketed products rely on this technology (Rapamune®, Emend®, TriCor® and Megace® ES are produced by media milling, whereas high-pressure homogenization is used for Triglide®). During media milling, nanosuspensions are produced by grinding a suspension of the drug and a suitable stabilizer in water with milling media such as yttrium-stabilized zirconium beads [5].

Nanoparticles are usually produced in liquid media, thereby forming a nanosuspension. There is, however, a general preference for solid oral dosage forms over liquid forms, for patient convenience and physical stability reasons [3]. As the primary objective of a nanoparticulate system is rapid dissolution, disintegration of the solid form and redispersion of the individual nanoparticles should be equally rapid, so that it does not impose a barrier on the overall dissolution process. Solidification methods for this transformation include pelletization, granulation, spray drying or lyophilization [3]. Prior to solidification, a matrix-former is often added to the suspension. Typical matrix-formers added prior to

* Corresponding author. Laboratory for Pharmacotechnology and Biopharmacy, K.U. Leuven, Gasthuisberg O&N2, Herestraat 49, Box 921, 3000 Leuven, Belgium. Tel.: +3216330304; fax: +3216330305.
E-mail address: Guy.VandenMooter@pharm.kuleuven.be (Van den Mooter Guy).

0939-6411/$ - see front matter © 2008 Elsevier B.V. All rights reserved.
doi:10.1016/j.ejpb.2008.06.007

drying are water-soluble sugars such as sucrose, lactose and mannitol, as adapted from freeze-drying [4]. In current literature, there is only a limited number of reports dealing with the transformation of nanosuspensions into solid products e.g. [6–10]. Reports focusing on the maintenance of the rapid dissolution characteristics obtained by nanosizing upon redispersion of the solid product in water are even more scarce e.g. [8].

This study focuses on the freeze-drying of TPGS-stabilized nanosuspensions. The model drug selected is itraconazole, a typical BCS class II compound having poor aqueous solubility which has already been used in nanoparticulate research in the past [11–12]. As dissolution was compromised due to freeze-drying, the need was identified to incorporate a matrix former. The traditional matrix-former sucrose was evaluated for this purpose. Since the effect of sucrose addition conflicted with what could be expected, its behavior during the freeze-drying process was further investigated. Finally, the use of microcrystalline cellulose (MCC, Avicel PH 101®) as an alternative matrix-former was evaluated, as MCC is a cheap excipient commonly applied as a binder/diluent in oral tablet and capsule technologies [13].

2. Materials and methods

2.1. Chemicals

Itraconazole, the yttrium-stabilized zirconium beads (diameter 0.5 mm) and colloidal silicon dioxide were kindly provided by Johnson & Johnson Pharmaceutical Research and Development (Beerse, Belgium). D-α-tocopherol polyethylene glycol 1000 succinate (TPGS, Eastman Chemical Company, Kingsport, TN, USA) was a gift from the manufacturer. D(+)-sucrose (Acros Organic, Geel, Belgium), microcrystalline cellulose (MCC, Avicel® PH 101, FMC Corporation, Cork, Ireland), acetonitrile gradient-grade far UV (Fisher Scientific UK Limited, Loughborough, UK), dimethylsulfoxide (Acros Organics, Geel, Belgium), methanol 99.9% for HPLC gradient-grade (Acros Organics, Geel, Belgium), sodium chloride (BDH Laboratory Supplies, Poole, UK), sodium laurylsulfate (Certa, Braine-l'Alleud, Belgium), tetrabutyl ammonium hydrogen sulfate (Acros Organics, Geel, Belgium), 1 M HCl (Titrinorm®, VWR International, Fontenay Sous Bois, France), sulfuric acid 95–97% (Merck, Darmstadt, Germany), anthrone (Merck, Darmstadt, Germany), Karl Fischer reagent 5 (Merck, Darmstadt, Germany) and disodium tartrate dihydrate (Merck, Darmstadt, Germany) were commercially obtained. Demineralized water was used for all experiments (Elga, maxima ultra pure water, $\geqslant$18 MΩ).

2.2. Nanosuspension production

Twenty grams of itraconazole, 2 g of TPGS 1000 (10% relative to the weight of itraconazole) and 100 ml of water were mixed and transferred into a grinding bowl (total bowl volume 335 ml). Subsequently, 300 g of yttrium-stabilized zirconium beads (ø 0.5 mm) were added, the grinding bowl was placed in the ball mill (Pulverisette 601, Fritsch GmbH, Idar Oberstein, Germany) and milling was initiated (clockwise, maximum intensity). After 15, 30, 60, 90, 120, 180, 240, 300 and 480 min, a sample was withdrawn (0.5 ml) and analyzed with dynamic light scattering (DLS) and laser diffractometry (LD) as presented in Sections 2.3 and 2.4, respectively. Subsequently, the nanosuspension was separated from the milling media by decanting the suspension, followed by the washing of the beads with water. Finally, the content of itraconazole in the nanosuspensions was determined by high-performance liquid chromatography (HPLC), as outlined in Section 2.5. In total, four batches were produced.

2.3. Dynamic light scattering (DLS)

DLS experiments were carried out on an ALV-NIBS High Performance Particle Sizer (ALV GmbH, Langen, Germany) equipped with a He–Ne laser with approximately 3 mW output at 632.8 nm, a digital correlator (ALV-5000/EMultiple Tau Digital correlator) and a single photon detector module (PMT). Detection was carried out in a backscattering mode (scattering angle 173°). Sample temperature was set at 25 °C. For each sample, 20 μl of sample was diluted with 1 ml of water in a cuvette and 10 runs of 10 s were performed. A 2nd order analysis was performed to calculate the mean particle size. The viscosity value used for calculations was 0.89 mPa.s.

2.4. Laser diffractometry (LD)

Laser diffractometry was performed on a Mastersizer Micro Plus (Malvern Instruments Limited, Worcestershire, UK) which has a working range of 0.050–550 μm. Analysis of the diffraction patterns was done using the Mie model ("standard" presentation: dispersant refractive index = 1.33, real particle refractive index = 1.5295, imaginary particle refractive index = 0.1). From the resulting volume distributions, the median was calculated (=50% volume percentile, $d_{(v,0.5)}$). All measurements were performed in triplicate.

2.5. Quantification of itraconazole by high-performance liquid chromatography (HPLC)

Samples were analyzed by HPLC on a Merck-Hitachi-Lachrom instrument (Hitachi Ltd., Tokyo, Japan) using a Merck Purospher® STAR RP-18 (150–4.6 mm; 5 μm) column (Merck, Darmstadt, Germany). A mobile phase consisting of 0.01 M tetrabutyl ammonium hydrogen sulfate in water and acetonitrile (50/50% (v/v)) was used. The flow rate was set at 1 ml/min and UV-detection was performed at 260 nm. The injection volume was 10 μl. A calibration curve with standards of 0.02–0.001 mg/ml in methanol was used. LOD was 0.2 μg/ml and LOQ 0.8 μg/ml.

For the determination of the content of itraconazole in the nanosuspension batches, described in Section 2.2 100 μl of nanosuspension was diluted to 100 ml with methanol. Subsequently, the resulting solution was diluted tenfold with methanol. The itraconazole content of each batch was determined in triplicate and the average was used for further calculations. Samples from dissolution experiments, presented in Section 2.12, were diluted fivefold with methanol prior to HPLC analysis. Analysis was performed in duplicate.

2.6. Quantification of sucrose by the anthrone assay

For the determination of the sucrose content in the dissolution samples, the anthrone assay was used [14]. Samples of 0.5 ml were mixed with 1.00-ml anthrone reagent 0.2% (w/v) in concentrated sulfuric acid. Due to the exothermic enthalpy of mixing, the sample was heated to its boiling point. The boiling mixture was then cooled to room temperature. After 45 min, the sample was vortexed and 200 μl of the sample was transferred to a flat transparent 96-well plate (Greiner Bio-One International AG, Frickenhausen, Germany). The plates were analyzed with a Tecan infinite 200 plate reader (Tecan Austria GmbH, Grödig/Salzburg, Austria) at 630 nm. For every plate, a 7-point calibration curve was determined (range 0.25–0.0025 mg/ml in dissolution medium). LOD was 0.9 μg/ml and LOQ 3 μg/ml. Each determination was performed in duplicate.

2.7. Quantification of water by the Karl Fischer assay

Water content of the samples during freeze-drying was determined, using the Karl Fischer assay. Measurements were per-

formed on a titration device (701 KF Titrino, Metrohm Ltd., Herisau, Switzerland) in methanol. Water content of the samples was measured after determination of the titer of the Karl Fischer reagent with disodium tartrate dihydrate (in triplicate, RSD 1.67%).

2.8. Freeze-drying of nanosized and non-nanosized formulations

2.8.1. Standard procedure

A volume of the itraconazole nanosuspensions corresponding to 1.5-g itraconazole, produced according to Section 2.2, was transferred into a 100-ml vial and sucrose or MCC was added (0%, 50%, 100% or 200% relative to the weight of itraconazole). Subsequently, water was added to obtain a suspension containing 90% (w/w) water (or 10% (w/w) itraconazole, TPGS 1000 and sucrose/MCC). Thereafter, the suspensions were frozen by immersing the vials in liquid nitrogen. Freeze-drying of the products was performed with a Christ model Alpha freeze-dryer (type 1050, Van Der Heyden, Brussels, Belgium) at a shelf temperature of −50 °C with a pressure below 1 mbar and the vials were removed after 48 h of drying. The same procedure was repeated for non-nanosized suspensions, starting from 1.5 g of unmilled itraconazole. Each formulation was produced in triplicate.

2.8.2. Deviations from the standard procedure

For the study of the influence of the freezing rate on nanoparticle agglomeration in the sucrose-based system, the suspension was frozen in a freezer at −28 °C (to obtain a lower freezing rate) or the suspension was injected directly in to a vessel containing liquid nitrogen with a syringe and needle (to obtain an ultra high-freezing rate). One batch was prepared for each freezing-rate condition.

For the evaluation of the effect of suspension dilution on nanoparticle agglomeration during freezing, suspensions containing 95% and 92% of water were prepared and frozen by immersing the vials in liquid nitrogen. One batch was produced for each dilution.

For the study of agglomeration during freeze-drying, 2-ml suspensions were prepared and freeze-dried. Samples were removed from the freeze-drying device after 4 or 24 h of drying and homogenized. Immediately thereafter, the samples were evaluated with Karl Fischer, differential scanning calorimetry (DSC), X-ray powder diffraction (XRPD) and LD, as presented in Sections 2.7, 2.10, 2.9 and 2.4, respectively.

2.9. X-ray powder diffraction (XRPD)

X-ray powder diffraction was performed at room temperature with an automated X'Pert PRO diffractometer (PANalytical, the Netherlands) in Bragg-Brentano geometry with a flat sample stage spinning with a rotation time of 4 s. X'Pert Data Collector version 2.2 c (PANalytical, the Netherlands) was used for data collection. In the incident beam path a 0.04-rad soller slit, a 10 mm mask and a programmable divergence slit were installed. In the diffracted beam path, a programmable anti scatter slit and a 0.04 rad soller slit were installed. CuKα_1-radiation (λ = 1.540598 Å) was obtained with a 0.02 mm Ni-filter. The irradiated and observed area was 100 mm^2. The irradiated and the observed length was 10 mm. The diffracted beams were detected with an X'celerator RTMS detector with an active length of 2.122° 2θ. The data were collected in continous mode in the region of $4° \leqslant 2\theta \leqslant 40°$ with a step size of 0.0021° 2θ and a counting time of 19.7 s. The X-ray tube was set up at a voltage of 45 kV and a current of 40 mA. The diffractograms were analyzed using X'pert Data Viewer version 1.2a.

2.10. Differential scanning calorimetry (DSC)

The DSC measurements were performed using a DSC Q1000 (TA Instruments, New Castle, USA) equipped with an intercooler. Data were treated mathematically using the resident Universal Analysis® Software. Calibration for temperature and heat of fusion was carried out with indium and octadecane as reference materials. The samples were analyzed in open aluminum pans and scanned under a nitrogen purge with a heating rate of 10 °C/min from 20 to 200 °C (n = 3).

2.11. Scanning electron microscopy (SEM)

SEM-studies were performed on a Philips XL30 SEM-FEG (FEI, Eindhoven, the Netherlands) equipped with a Schottky Field-emission electron gun (FEG). Prior to imaging, mounted samples were sputter-coated with gold during 45 s (Sputtering device 07 120; Balzers Union, Liechtenstein). A 10-kV electron beam was used and detection was performed with a conventional Everhart–Thornley secondary electron detector.

2.12. Dissolution experiments

Dissolution experiments were performed using an SR8 PLUS instrument (Hanson Research Corporation, Chatsworth, CA, USA). 500-ml medium containing 2 g/l sodium laurylsulfate, 0.084 M HCl and 2 g/l sodium chloride was selected as a dissolution medium to ensure complete solubility of itraconazole. Dissolution was performed at 37 °C, using a paddle speed of 100 rpm. The amount of sample for each experiment was equivalent to 50 mg of itraconazole. Samples of 5 ml were taken after 1.5, 3, 6, 15, 30, 60, 90 and 120 min and were filtrated through a 0.1-μm PTFE syringe filter (Whatman Inc., Clifton, NJ, USA). Subsequently, 5 ml of fresh medium was added to the dissolution vessel. Quantification of the samples was done by HPLC, as described in Section 2.5. The necessary corrections for the amount of sample removed from the vessel were made in further calculations. Each formulation tested was evaluated in triplicate and for each individual profile, the Weibull shape parameter (b) and scale parameter (a) were calculated, from which the dissolution time (T_d, time interval necessary to release 63.2% of the drug) was derived [15–16]. For the calculation of the different parameters, the maximal observed release value was used in case a plateau was observed in the dissolution profile. Otherwise, a value of 100% was applied. Exclusion of the 1.5- and 3-min points and the points above 90% of release was allowed as it is known that small deviations in the lower and upper parts of dissolution curves can be extremely overemphasized after Weibull linearization [16]. A minimum of four time points were used for analysis and the R^2 value of the fitted curve was always higher than 0.97.

3. Results and discussion

3.1. Nanosuspension production and freeze-drying without additional matrix-formers

Particle-size properties after media milling of itraconazole are provided in Fig. 1A. DLS showed a reduction of the average particle diameter to 337 ± 74 nm after 480 min of milling, while LD resulted in an average diameter of 435 ± 48 nm. The average LD particle-size distribution (Fig. 1B) of the non-nanosized products showed a bimodal distribution with maxima at 0.4 and 6.6 μm. After milling, apart from a global maximum at 0.4 μm, a small local maximum could be observed at 4.2 μm. The SEM picture of the freeze-dried product (Fig. 1C, 35000×) clearly revealed a porous submicron structure. XRPD spectra of a non-nanosized and nanosized freeze-dried product are provided in Fig. 2. together with the results for pure itraconazole and TPGS 1000. Crystalline itraconazole could be easily seen in both the non-nanosized and the nanosized product, which is positive in terms of physical stability

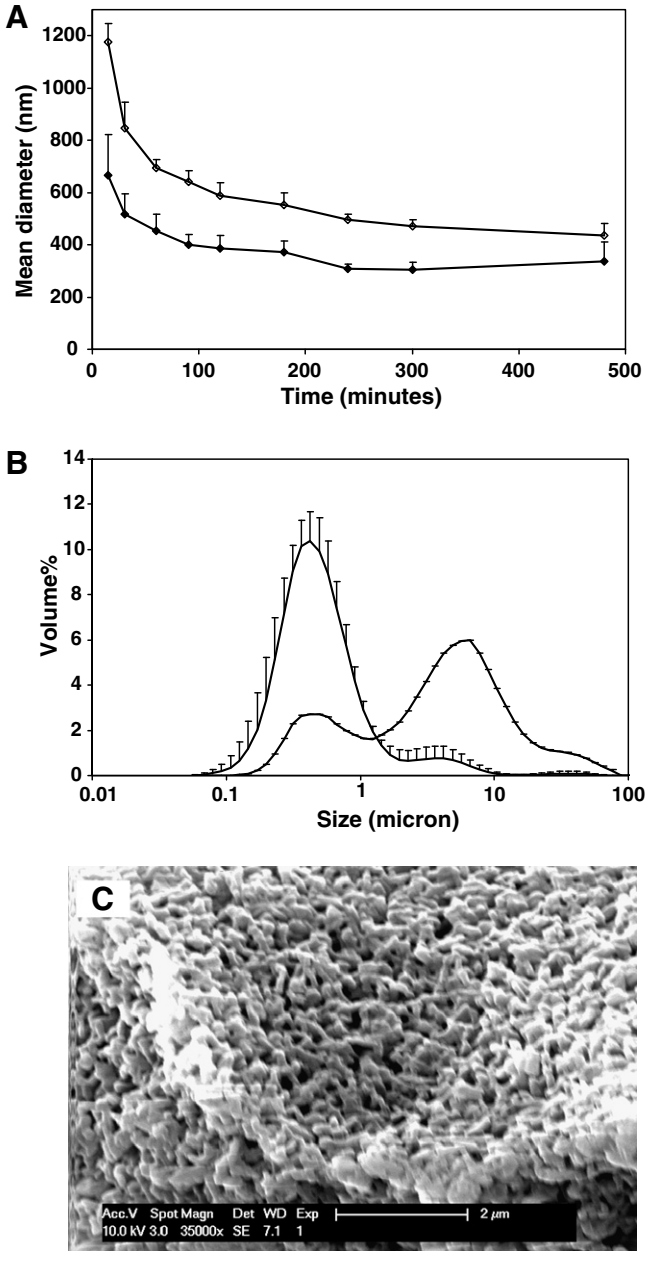

Fig. 1. Milling monitoring of the scale-up batches ($n = 4$): (A) gradual decrease of the particle size by DLS (♦) and LD (◇), (B) LD particle size of the nanosized product (left) and the starting product (right), (C) SEM picture (35000×): submicron-structure of the freeze-dried product. Error bars in A and B indicate the standard deviation of the obtained results.

of the product. The itraconazole peaks showed some peak broadening in the nanosized product that can originate from smaller particle sizes (crystallites) and/or from stress and strain due to the milling process. The polyethyleneglycol diffraction peaks of TPGS could be observed in both spectra, although overlaping with itraconazole peaks occurs. Representative DSC-thermograms are provided in Fig. 3. The itraconazole melting peak tended to shift to a lower temperature in the nanosized products (158.2 ± 0.4 °C), compared to the non-nanosized freeze-dried products and pure itraconazole [162.4 ± 0.2 and 165.1 ± 0.1, respectively], a feature that might be due to smaller itraconazole crystals, as given by the Gibbs–Thomson equation [17]. Both in the non-nanosized and in the nanosized products, a weak TPGS melting signal could be distinguished.

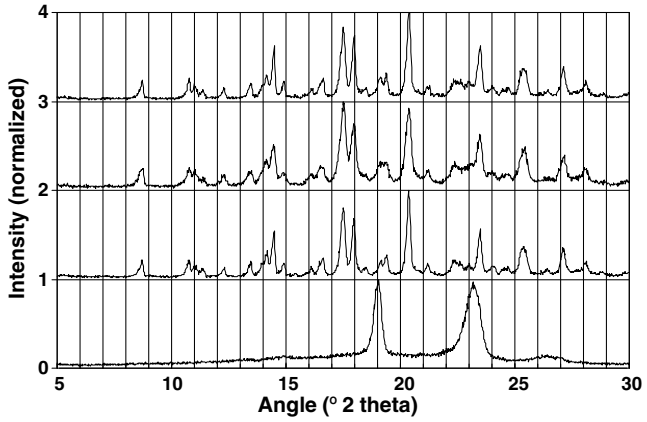

Fig. 2. XRPD-spectra: from top to bottom: non-nanosized freeze-dried powder, nanosized freeze-dried powder, pure itraconazole, TPGS 1000.

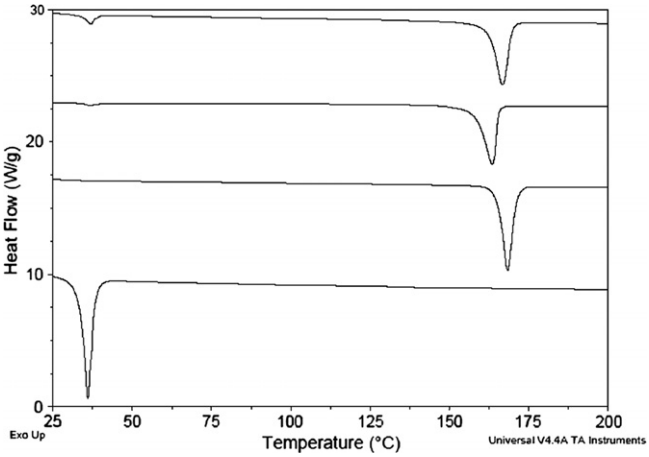

Fig. 3. Representative DSC-thermograms: from top to bottom: non-nanosized freeze-dried powder, nanosized freeze-dried powder, pure itraconazole, TPGS 1000.

Dissolution results of the nanosized and non-nanosized suspensions and freeze-dried products are provided in Fig. 4. They clearly demonstrate the beneficial effect of nanosizing on the dissolution rate. The time required for 63.2% of release (T_d) for all dissolution

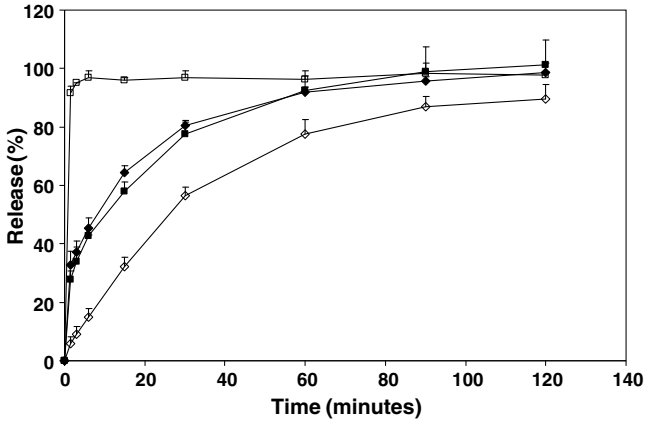

Fig. 4. Dissolution profiles for the products without additional excipients ($n = 3$): □ nanosuspension, ■ starting suspension, ◇ freeze-dried nanosuspension, ♦ freeze-dried starting suspension.

Table 1
Summary of the T_d values (time to release 63.2%) as obtained through Weibull linearization of the dissolution profile

ID	Sample	T_d (63.2% release) (min)
A	Nanosized suspension	<1.5[a]
B	Non-nanosized suspension	16.9 ± 2.4
C	Freeze dried powder, non-nanosized	12.3 ± 0.2
D	Freeze dried powder, nanosized	42.0 ± 6.9
E	Freeze dried powder, non-nanosized, 50% sucrose[b]	11.1 ± 0.9
F	Freeze dried powder, non-nanosized, 100% sucrose[b]	11.5 ± 2.0
G	Freeze dried powder, non-nanosized, 200% sucrose[b]	10.1 ± 1.1
H	Freeze dried powder, nanosized, 50% sucrose[b]	22.7 ± 8.7
I	Freeze dried powder, nanosized, 100% sucrose[b]	40.1 ± 8.3
J	Freeze dried powder, nanosized, 200% sucrose[b]	209.2 ± 178.9
K	I, ultra rapid freezing by injection in liquid N_2	53.4 ± 10.5
L	I, slow freezing in freezer @ −28 °C	45.7 ± 3.6
M	I, diluted to 5% solids prior to freezing	54.9 ± 23.5
N	I, diluted to 2% solids prior to freezing	43.3 ± 2.2
O	Freeze dried powder, non-nanosized, 50% MCC[b]	19.0 ± 2.2
P	Freeze dried powder, non-nanosized, 100% MCC[b]	20.7 ± 0.3
Q	Freeze dried powder, non-nanosized, 200% MCC[b]	15.9 ± 2.4
R	Freeze dried powder, nanosized, 50% MCC[b]	10.5 ± 0.7
S	Freeze dried powder, nanosized, 100% MCC[b]	6.4 ± 1.2
T	Freeze dried powder, nanosized, 200% MCC[b]	3.1 ± 0.5

[a] Weibull analysis was not possible as all data points showed more than 90% release.
[b] Percentages mentioned are relative to the weight of itraconazole.

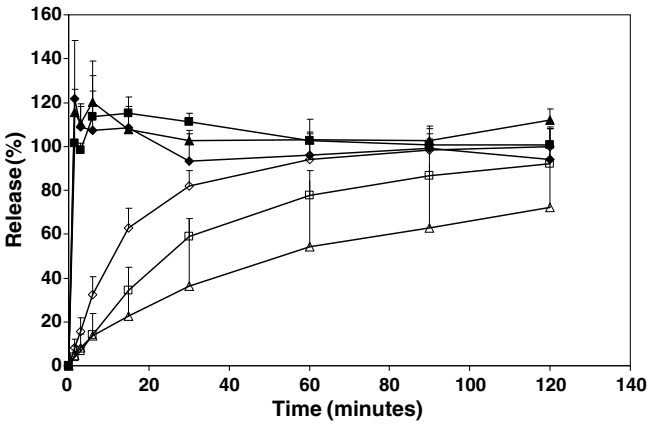

Fig. 5. Dissolution profiles for sucrose and itraconazole in the nanosized products ($n = 3$): ♦ sucrose-50% formulation, ◇ itraconazole-50% formulation, ■ sucrose-100% formulation, □ itraconazole-100% formulation, ▲ sucrose-200% formulation and Δ itraconazole-200% formulation.

experiments is listed in Table 1 For the non-nanosized suspension, the T_d was 16.9 ± 2.4 min, whereas for the nanosuspension, no T_d could be calculated, as more than 90% was already dissolved after 1.5 min Table 1A–B). The T_d (Table 1C–D) for the freeze-dried non-nanosized product was a bit lower than for the original suspension, demonstrating that dissolution is not compromised by freeze-drying. For the freeze-dried nanosized product, however, dissolution (T_d = 42.0 ± 6.9 min) was slower than for the nanosuspension and the non-nanosized products. The underlying reason for this dissolution behavior is agglomeration of the nanoparticles during freeze-drying. These results clearly underline the need for the addition of a matrix-former to these nanosuspensions prior to freeze-drying, in order to preserve the dissolution advantage offered by nanosizing.

3.2. Freeze-drying with sucrose as a matrix-former

As previous results indicated the need to add a matrix-former prior to freeze-drying, the traditional freeze-drying excipient sucrose was added in amounts of 50%, 100% and 200% relative to the weight of itraconazole. For the non-nanosized formulations (Table 1E–G), the T_d was comparable for the different formulations and similar to the results obtained for the freeze-dried product without sucrose. For the nanosized formulations (Table 1H–J), dissolution was always slower compared to the non-nanosized formulations. Contrary to what would be intuitively expected, adding a higher amount of sucrose slowed down dissolution [T_d = 42.0 ± 6.9 min (0%), 22.7 ± 8.7 min (50%), 40.1 ± 8.3 min (100%) and 209.2 ± 178.9 min (200%)]. Furthermore, a large inter-batch variability could be observed for products with the same content, as displayed by the standard deviations of the T_d's. To obtain further insight into these unexpected results, a number of additional experiments were performed on the nanosized formulations.

First, the possibility of altered sucrose dissolution due to the other powder constituents was evaluated. Therefore, the dissolution of both sucrose and itraconazole was monitored for the different formulations. Dissolution profiles are provided in Fig. 5. The results show that the dissolution of sucrose was very rapid in all of the formulations and it is in line with what can be expected from the Noyes–Withney equation, given the high solubility of sucrose in water.

Subsequently, nanoparticle agglomeration was evaluated. Indeed, for powders containing higher amounts of sucrose, larger agglomerates were observed [LD average diameters: 69.8 ± 7.7 μm (0%), 55.4 ± 26.7 μm (50%), 128.2 ± 7.8 μm (100%) and 219.1 ± 154.1 μm (200%)]. Hence, the key question is exactly *when* this agglomeration occurs during the freeze-drying process.

A first possibility is that the sucrose in the suspensions could trigger agglomeration of the nanoparticles prior to freezing of the suspension. To test this possibility, identical suspensions were prepared as those originally prepared for freeze-drying and short-term physical stability (8 h of storage at ambient conditions) was assayed. From these experiments, it was found that no increase in particle size could be observed in any of the nanosuspensions [LD average diameters: 0.38 ± 0.03 μm (0%), 0.38 ± 0.02 μm (50%), 0.35 ± 0.02 μm (100%) and 0.36 ± 0.03 μm (200%)]. Thus, nanoparticle agglomeration during storage prior to freezing was not a valid scenario. Secondly, it was questioned whether freezing of the nanosuspension could cause agglomeration. The influence of freezing on the agglomeration of nanosized systems has been reported before for systems such as lipid/DNA complexes e.g. [18], PEGylated nanoparticles e.g. [19], proteins e.g. [20] and nanoparticles e.g. [21]. In the latter, agglomeration of the drug nanocrystals tended to decrease in lower concentrated systems and when faster freezing rates were employed. Therefore, both strategies were evaluated on the formulation with 100% sucrose in order to prevent or reduce agglomeration of the nanoparticles. The influence of a higher freezing-rate was tested by directly transferring the suspension into liquid nitrogen with a needle and syringe. Slower freezing was obtained by freezing the vial in a freezer at −28 °C. The effect of concentration was investigated by using nanosuspensions containing 2% and 5% of solids (in stead of 10%). T_d's for the dissolution profiles are summarized in Table 1K–N and these indicate no significant differences between the different freezing procedures. As the observed results were not in line with what would be expected, the influence of freeze-drying was investigated in more detail. To study separately the influence of freezing from that of drying, suspensions identical to those originally prepared were frozen in liquid nitrogen, left to thaw at room temperature and particle size was determined using LD. The results confirm that adding higher amounts of sucrose had a protective effect on nanoparticle agglomeration dur-

ing the freezing process [LD average diameters: 23.1 ± 0.5 μm (0%), 11.6 ± 0.3 μm (50%), 7.6 ± 0.1 μm (100%) and 1.3 ± 0.1 μm (200%)].

Intriguingly, although protective during freezing, sucrose seems to induce agglomeration during subsequent drying. Samples removed during freeze-drying of suspensions with 100% sucrose provide further insight in to this agglomeration process. After removal of 68% of the water, the product was still a suspension when allowed to thaw. LD average diameter was 7.1 ± 0.3 μm, a value similar to the one obtained after freezing and thawing (7.6 ± 0.1 μm), indicating that no further agglomeration had occurred. When all of the water was removed (99.9%), on the other hand, the measured LD average diameter was 74.3 ± 7.1 μm, close to the final value of 128.2 ± 7.8 μm. Interestingly, amorphous sucrose was confirmed both by DSC (amorphous sucrose has a characteristic cold crystallization exotherm around 140 °C [8], data not shown) and XRPD (no sucrose diffraction peaks in the spectrum, data not shown). Therefore, it is not the subsequent conversion of amorphous sucrose to its crystalline state (as seen with XRPD and DSC, data not shown) that triggers agglomeration.

3.3. Freeze-drying with microcrystalline cellulose as a water-insoluble matrix-former

It was clear from the previous results that the agglomeration of itraconazole nanoparticles in the freeze-dried product could not be prevented by using sucrose as a matrix-former. Therefore, an alternative matrix-former was evaluated. The water-insoluble matrix-former microcrystalline cellulose (MCC) was added to the suspensions in order to prevent agglomeration of the nanoparticles during freeze-drying. Particle size of the grade used is 66.7 ± 0.1 μm (Avicel PH 101®, measured with LD). Dissolution experiments for nanosized and non-nanosized systems containing 50%, 100% and 200% MCC were performed and are summarized in Table 1O–T. As for the sucrose-based products, no big differences could be seen for the non-nanosized systems. For the nanosized powders, however, fast dissolution was observed and higher amounts of MCC resulted in higher dissolution rates [T_d = 42.0 ± 6.9 min (0%), 10.5 ± 0.7 min (50%), 6.4 ± 1.2 min (100%) and 3.1 ± 0.5 min (200%)]. The dissolution profiles of the nanosized powders are given in Fig. 6. From these profiles, two phases can be distinguished: an initial burst dissolution, followed by a phase of slower dissolution of the remaining product. While the former is clearly an effect of the dissolution of individual nanoparticles, the latter indicates an agglomerated fraction of nanoparticles. Interestingly, the fraction showing burst release increased upon using higher amounts of MCC, clearly demonstrating the potential of MCC as a matrix-former. The fact that MCC is a water-insoluble product might be responsible for this behavior. Being so, it forms a permanent barrier for nanoparticle agglomeration. The observed agglomeration data suggest that this barrier is not permanent in the case of sucrose. During freeze-drying, the latter system evolves from a sucrose solution to a concentrated solution that is then transformed into a hygroscopic, glassy state that finally crystallizes out [for more details on the amorphous to crystalline conversion of sucrose in these types of systems, the reader is suggested to consult (8) and references therein]. Apparently, due to these complex changes, the sucrose system is unable to form a permanent barrier for itraconazole nanoparticle agglomeration. The fact that a water-insoluble product like MCC does not behave as complex during the drying process might explain the observed better performance of MCC as a matrix-former. Evaluation of alternative water-insoluble matrix-formers for nanosuspension-drying purposes is the subject of a follow-up study.

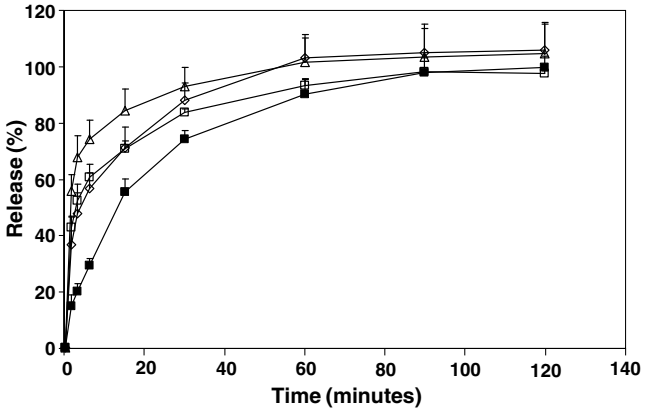

Fig. 6. Dissolution profiles for formulations containing MCC (n = 3): ◇ nanosized powder 50% MCC, □ nanosized powder 100% MCC, Δ nanosized powder 200% MCC and ■ non-nanosized powder 100% MCC.

4. Conclusion

Itraconazole nanosuspensions containing 10% TPGS 1000 (337 ± 74 nm, DLS) showed complete dissolution within minutes. As these dissolution characteristics could not be obtained upon freeze-drying of the nanosuspension due to agglomeration, two different matrix-formers were evaluated in amounts of 50%, 100% and 200% (relative to the weight of itraconazole). For the traditional water-soluble matrix-former sucrose, higher amounts of sucrose unexpectedly decreased the dissolution rate [T_d = 42.0 ± 6.9 min (0%), 22.7 ± 8.7 min (50%), 40.1 ± 8.3 min (100%), 209.2 ± 178.9 min (200%)]. Although higher amounts of sucrose clearly had a cryoprotective effect on nanoparticle agglomeration, substantial agglomeration could be observed during the final part of the drying process. As a result, an overall negative effect of higher sucrose amounts was seen. For microcrystalline cellulose (MCC), higher amounts resulted in faster dissolution [T_d = 42.0 ± 6.9 min (0%), 10.5 ± 0.7 min (50%), 6.4 ± 1.2 min (100%) and 3.1 ± 0.5 min (200%)]. Two distinct phases could be distinguished in these dissolution profiles, an initial phase of burst release due to the individually dispersed nanoparticles and a phase of slower release that can be ascribed to an agglomerated drug fraction. The data clearly demonstrate the efficiency of MCC as a viable alternative for the preservation of the dissolution-rate advantage of the nanoparticles upon freeze-drying.

Acknowledgements

The authors thank Rudy De Vos for support during the electron microscopy experiments, professor Jos Hoogmartens and Ward D'Autry for making the Karl Fischer determinations possible. The work was carried out within the framework of an interdisciplinary research project sponsored by K.U. Leuven (IDO-project IDO/04/009). The authors acknowledge financial support from FWO-Vlaanderen (G.0614.07).

References

[1] C. Lipinski, Poor aqueous solubility – an industry wide problem in drug discovery, Am. Pharm. Rev. 5 (2002) 82–85.
[2] B.E. Rabinow, Nanosuspensions in drug delivery, Nat. Rev. Drug Discov. 3 (2004) 785–796.
[3] R.H. Müller, J. Möschwitzer, F.N. Bushrab, Manufacturing of nanoparticles by milling and homogenization techniques, in: R.B. Gupta, U.B. Kompella (Eds.), Nanoparticle technology for drug delivery, Drugs and the Pharmaceutical Sciences, vol. 159, Taylor & Francis Group, LLC, NewYork, USA, 2006, pp. 21–51.
[4] F. Kesisoglou, S. Panmai, Y. Wu, Nanosizing – oral formulation development and biopharmaceutical evaluation, Adv. Drug Deliv. Rev. 59 (2007) 631–644.

[5] V.B. Patravale, A.A. Date, R.M. Kulkarni, Nanosuspensions: a promising drug delivery strategy, J. Pharm. Pharmacol. 56 (2004) 827–840.
[6] G.J. Vergote, C. Vervaet, I. Van Driesche, S. Hoste, S. De Smedt, J. Demeester, R.A. Jain, S. Ruddy, J.P. Remon, An oral controlled release matrix pellet formulation containing nanocrystalline ketoprofen, Int. J. Pharm. 219 (2001) 81–87.
[7] J. Möschwitzer, R.H. Müller, Spray coated pellets as carrier system for mucoadhesive drug nanocrystals, Eur. J. Pharm. Biopharm. 62 (2006) 282–287.
[8] B. Van Eerdenbrugh, L. Froyen, J.A. Martens, N. Blaton, P. Augustijns, M. Brewster, G. Van den Mooter, Characterization of physico-chemical properties and pharmaceutical performance of sucrose co-freeze-dried solid nanoparticulate powders of the anti-HIV agent loviride prepared by media milling, Int. J. Pharm. 338 (2007) 198–206.
[9] J. Lee, Drug nano- and microparticles processed into solid dosage forms: physical properties, J. Pharm. Sci. 92 (2003) 2057–2068.
[10] Y.N. Konan, R. Gurny, E. Allémann, Preparation and characterization of sterile and freeze dried sub-200 nm nanoparticles, Int. J. Pharm. 233 (2002) 239–252.
[11] J.W. Mouton, A. van Peer, K. de Beule, A. Van Vliet, J.P. Donnelly, P.A. Soons, Pharmacokinetics of itraconazole and hydroxyitraconazole in healthy subjects after single and multiple doses of a novel formulation, Antimicrob. Agents Chemother. 50 (2006) 4096–4102.
[12] J.M. Vaughn, J.T. McConville, D. Burgess, J.I. Peters, K.P. Johnston, R.L. Talbert, R.O. Williams III, Single dose and multiple dose studies of itraconazole nanoparticles, Eur. J. Pharm. Biopharm. 63 (2006) 95–102.
[13] P.J. Weller, Cellulose microcrystalline, in: R.C. Rowe, P.J. Sheskey, P.J. Weller (Eds.), Handbook of Pharmaceutical Excipients, Fourth ed., Pharmaceutical Press, London, UK, 2003, pp. 108–111.
[14] A.J. Scott, E.H. Melvin, Determination of dextran with anthrone, Anal. Chem. 25 (1953) 1656–1661.
[15] P. Costa, J.M.S. Lobo, Modeling and comparison of dissolution profiles, Eur. J. Pharm. Sci. 13 (2001) 123–133.
[16] F. Langenbucher, Linearization of dissolution rate curves by the Weibull distribution, J. Pharm. Pharmacol. 24 (1972) 979–981.
[17] C.L. Jackson, G.B. McKenna, The melting behavior of organic materials confined in porous solids, J. Chem. Phys. 93 (1990) 9002–9011.
[18] S.D. Allison, M.d.C. Molina, T.J. Anchordoquy, Stabilization of lipid/DNA complexes during the freezing step of the lyophilization process: the particle isolation hypothesis, Biochim. Biophys. Acta 1468 (2000) 127–138.
[19] W.L.J. Hinrichs, F.A. Manceñido, N.N. Sanders, K. Braeckmans, S.C. De Smedt, J. Demeester, H.W. Frijlink, The choice of a suitable oligosaccharide to prevent aggregation of PEGylated nanoparticles during freeze thawing and freeze drying, Int. J. Pharm. 311 (2006) 237–244.
[20] J.D. Engstrom, E.S. Lai, B.S. Ludher, B. Chen, T.E. Milner, R.O. Williams, G.B. Kitto, K.P. Johnston, Formation of stable submicron protein particles by thin film freezing, Pharm. Res. 25 (2008) 1334–1346.
[21] J. Lee, Y. Cheng, Critical freezing rate in freeze drying nanocrystal dispersions, J. Control. Release 111 (2006) 185–192.